Nuclear Engineering and Technology 53 (2021) 2803–2815

Contents lists available at ScienceDirect

Nuclear Engineering and Technology

journal homepage: www.elsevier.com/locate/net

Original Article

Uncertainty quantification in decay heat calculation of spent nuclear fuel by STREAM/RAST-K

Jaerim Jang, Chidong Kong, Bamidele Ebiwonjumi, Alexey Cherezov, Yunki Jo, Deokjung Lee*

Department of Nuclear Engineering, Ulsan National Institute of Science and Technology, 50 UNIST-gil, Ulsan, 44919, Republic of Korea

ARTICLE INFO

Article history:
Received 15 September 2020
Received in revised form
31 January 2021
Accepted 8 March 2021
Available online 15 March 2021

Keywords:
PWR
Decay heat
Spent nuclear fuel
Uncertainty quantification
Back-end cycle

ABSTRACT

This paper addresses the uncertainty quantification and sensitivity analysis of a depleted light-water fuel assembly of the Turkey Point-3 benchmark. The uncertainty of the fuel assembly decay heat and isotopic densities is quantified with respect to three different groups of diverse parameters: nuclear data, assembly design, and reactor core operation. The uncertainty propagation is conducted using a two-step analysis code system comprising the lattice code STREAM, nodal code RAST-K, and spent nuclear fuel module SNF through the random sampling of microscopic cross-sections, fuel rod sizes, number densities, reactor core total power, and temperature distributions. Overall, the statistical analysis of the calculated samples demonstrates that the decay heat uncertainty decreases with the cooling time. The nuclear data and assembly design parameters are proven to be the largest contributors to the decay heat uncertainty, whereas the reactor core power and inlet coolant temperature have a minor effect. The majority of the decay heat uncertainties are delivered by a small number of isotopes such as ^{241}Am, ^{137}Ba, ^{244}Cm, ^{238}Pu, and ^{90}Y.

1. Introduction

This paper presents the uncertainty quantification (UQ) of the decay heat for a pressurization water reactor (PWR) fuel assembly (FA) using the STREAM/RAST-K two-step method. The importance of the intermediate storage facility design and management of the spent fuel assembly is increasing as the saturation issue of the spent fuel pool (SFP) continues to increase. According to a recent report [1], the SFP of the Kori nuclear power plant Units 1–4 (in South Korea) will be completely saturated by 2024. To ensure the safety of spent nuclear fuel (SNF) management and transport, an accurate code system is necessary. The evaluation of the decay heat uncertainty is essential to assess the reliability of the developed code system for the prediction of decay heats. In addition, UQ is required to provide the design margin for the SNF cask, licensing analysis of the developed code system, and to provide the information to SNF applications [2].

The developed calculation module has been adopted in the STREAM/RAST-K two-step method and validated with 58 SNFs [3,4]. RAST-K SNF was developed to reduce the calculation time using Lagrange interpolation instead of solving the micro-depletion chain and without using an additional code system for the back-end cycle analysis [4]. As a follow-up study, this paper presents the UQ of decay heat with three different groups of diverse parameters: neutronics data, FA design parameters, and operating conditions of the 3D core simulation. A stochastic sampling method is used for the uncertainty calculation with 500 perturbed two-group cross-section data and number-density files.

The stochastic sampling method has been used to assess the uncertainty of different developed code systems: CASMO [5], MCNP [6,7], SCALE [2], and SERPENT [7]. The UQ of CASMO-5 was performed with cross-section covariance data from ENDF/B-VII.1 (162 isotopes) [8] and from the SCALE-6.0 variance-covariance matrix (399 isotopes) [9]. In addition, a UQ study of a Monte Carlo code, MCNP (version 4C3), was calculated with basic cross-section covariance data coupled with isotope inventory code ACAB [6,10]. Moreover, the UQ study of SCALE6.2.1 was performed with the ENDF/B-VII.1 covariance data of 187 isotopes based on 6432R1 FA discharged from a boiling water reactor (BWR) [2]. The majority of the analyses (CASMO-5, MCNP4C3, and SERPENT) focused on the evaluation of isotope uncertainty caused by neutronics data (*i.e.*, cross-section library and fission yield data) [2]. A small number of

* Corresponding author.
E-mail address: deokjung@unist.ac.kr (D. Lee).

https://doi.org/10.1016/j.net.2021.03.010

the published results (including Reference [2]) focused on the analysis of the decay heat uncertainty caused by the operating conditions, design parameters, and neutronics data. This paper addresses the decay heat uncertainty of the PWR FA type using Lagrange interpolation. The B-43 FA of Turkey Point-3 was used for the calculation.

This paper presents the items as follows, Section 2 details the code system to generate the cross-section library with covariance data and to calculate the decay heat; Section 3 presents the specification of the FA problems, and Section 4 presents and discusses the results of the UQ.

2. Code system

2.1. STREAM/RAST-K

The decay heat calculation is performed with a two-step method composed of in-house code, lattice code STREAM [14], and nodal code RAST-K v2.0 [3,15]. STREAM is implemented using the method of characteristics. Stamm'ler equivalence two-term method is used for the resonance treatment [16]. Two-group cross-section data and number-density files are generated by branch and history depletion branch calculations, separately.

RAST-K v2.0 is a nodal code implemented with multigroup coarse mesh finite difference (CMFD) acceleration and the multigroup unified nodal method (UNM) [3,15]. RAST-K SNF is implemented with Lagrange interpolation for the prediction of the isotope inventory and calculation of the decay heat [3,4]. The calculation module for the decay heat is implemented; this has been validated as indicated in Refs. [3,22]. The actinide isotopes of 22, fission product of 12, and burnable poison of 2 are calculated using the micro-depletion module of RAST-K [3]. The other 1604 isotopes are generated by the Lagrange interpolation method based on the number-density file produced by STREAM. Fixed temperature conditions are used to maintain consistency with the measurements [13]. The other conditions, boron concentration, specific power density, and effective full power day of cycle, are adjusted according to Reference [13].

2.2. Isotope inventory calculations

RAST-K calculates the inventory of 36 nuclides (presented in Table 3 of Reference [3]) using a micro-depletion solver [15]; the other 1604 isotopes are calculated by Lagrange interpolation [3,4,23]. To consider the cumulative condition of the 3D core simulation, three history indices are used. The history indices are the time-averaged values of the moderator temperature, fuel temperature, and boron concentration [3,4,23]. Ten history branches are used for interpolation; the cases are described in Table 1 of Reference [3].

Equation (1) displays the Lagrange interpolation equation [23]; the number density (ND) of ten history branch cases is used for the calculation. The conditions of indices 1 and 2–5 (displayed in Table I of Reference [3]) are used for the fourth-order Lagrange interpolation with a history index of the moderator temperature. Indices 1, 6, and 7 are used for the second-order Lagrange interpolation of the fuel temperature conditions. Indices 1 and 8–10 are used for the third-order Lagrange interpolation of the boron concentration. The detailed method is presented in Reference [3].

$$ND_{Lagrange} = \Delta ND_{TMO} + \Delta ND_{TFU} + \Delta ND_{BOR} + ND_1, \quad (1)$$

where ND is the number density, $ND_{Lagrange}$ is the total number density calculated by the Lagrange interpolation combined with the history indices; ΔND_{TMO} is the calculated number-density difference caused by the moderator temperature conditions between the reference case (Index 1) and history index (h_{TMO}); ΔND_{TFU} is the number-density difference caused by the fuel temperature, and ΔND_{BOR} is the difference caused by the boron concentration. The notation ND_1 represents the number density of the reference case. To consider the effect of different power levels during the core operation, a power correction factor is used to correct the calculated number density. The final result of the number density is calculated using Equation (2).

$$ND_{calculated} = ND_{Lagrange} * PCF, \quad (2)$$

where PCF is a power correction factor and is used to adjust the effect of different power levels in the operating conditions [3,24,25]. Equation (3) presents the formula for the decay heat calculation [3,22].

$$H = \sum N_i \lambda_i Q_i, \quad (3)$$

where H is the decay heat; the notation i is the isotope index; N is the number; λ is the decay constant, and Q is the total recoverable energy per decay [3,22].

2.3. Stochastic sampling method

STREAM generates a cross-section library with covariance data according to Reference [17] in three steps: (1) evaluation of the 72-group covariance matrix for the microscopic cross-section using NJOY-99 [17,18]. ENDF/B-VII.1 covariance data (144 isotopes as displayed in Table 1) are used herein [19] [20] [21]; (2) generation of the perturbed five hundred libraries; and (3) calculation of the 3D nodal simulation with perturbed two-group cross-sectional and number-density files. Fig. 1 presents the flow chart of the UQ. The ENDF/B-VII.0 decay library is used in this study [17]. The perturbed microscopic cross-section is generated by Equation (4) [17].

$$\mathbf{x} = \mathbf{A}\mathbf{z} + \boldsymbol{\mu}, \quad (4)$$

where $\mathbf{A}$ is an n by n matrix; n is the number of cross-section types; matrix $\mathbf{A}$ is calculated by the covariance data according to Equation (15) of Reference [17]. The data of $\mathbf{A}$ are generated by NJOY-99 [18]. Singular value decomposition is used to solve matrix **A;** the details are provided in Section II·C.2 of Reference [17]. Vector $\boldsymbol{\mu}$ is the mean vector and stores the unperturbed 72-group microscopic cross-sections [17]. Vector $\mathbf{z}$ is a multivariate standard normal random vector [17]. Vector $\mathbf{x}$ represents the perturbed 72-group microscopic cross-sections [17]. Five different types of cross-section covariance data are contained: total scattering (elastic and inelastic), fission, capture, number of generated neutrons per fission, and fission spectrum. Perturbation of the fission yield is not considered in this study.

The uncertainty of the neutron XS libraries is obtained by repeating the same calculation using different random number series (*i.e.*, random seeds). Library-1 is a neutronics dataset (composed of a number-density file and two-group XS data) perturbed with the first random seed. Core characteristic-1 is calculated by perturbed Library-1 (*i.e.*, paired perturbed number-density file and perturbed two-group XS dataset). Decay heat-1 is calculated by Core characteristic-1. As indicated in Fig. 1, the calculation results of the decay heat depend on the cross-section data and number-density files. Table 1 presents the list of perturbed isotopes

Table 1
Covariance isotope list.

ENDF/B-VII.1 (144)	^{1}H	^{2}H	^{4}He	^{6}Li	^{9}Be	^{10}B	^{11}B	C	^{15}N
	^{16}O	^{19}F	^{23}Na	^{24}Mg	^{27}Al	^{28}Si	^{29}Si	^{30}Si	^{46}Ti
	^{47}Ti	^{48}Ti	^{49}Ti	^{50}Ti	^{50}Cr	^{52}Cr	^{53}Cr	^{55}Mn	^{54}Fe
	^{56}Fe	^{57}Fe	^{59}Co	^{58}Ni	^{60}Ni	^{89}Y	^{90}Zr	^{91}Zr	^{92}Zr
	^{93}Zr	^{94}Zr	^{95}Zr	^{96}Zr	^{92}Mo	^{94}Mo	^{95}Mo	^{96}Mo	^{97}Mo
	^{98}Mo	^{100}Mo	^{99}Tc	^{109}Ag	^{133}Cs	^{135}Cs	^{141}Pr	^{143}Nd	^{145}Nd
	^{146}Nd	^{148}Nd	^{152}Gd	^{153}Gd	^{154}Gd	^{155}Gd	^{156}Gd	^{157}Gd	^{158}Gd
	^{160}Gd	^{180}W	^{182}W	^{183}W	^{184}W	^{186}W	^{191}Ir	^{193}Ir	^{197}Ir
	^{204}Pb	^{206}Pb	^{207}Pb	^{208}Pb	^{209}Pb	^{225}Ac	^{226}Ac	^{227}Ac	^{227}Th
	^{228}Th	^{229}Th	^{230}Th	^{231}Th	^{232}Th	^{233}Th	^{234}Th	^{229}Pa	^{230}Pa
	^{232}Pa	^{230}U	^{231}U	^{232}U	^{233}U	^{235}U	^{238}U	^{234}Np	^{235}Np
	^{236}Np	^{237}Np	^{238}Np	^{239}Np	^{236}Pu	^{237}Pu	^{238}Pu	^{239}Pu	^{240}Pu
	^{242}Pu	^{244}Pu	^{246}Pu	^{240}Am	^{241}Am	^{240}Cm	^{241}Cm	^{242}Cm	^{243}Cm
	^{244}Cm	^{245}Cm	^{246}Cm	^{247}Cm	^{248}Cm	^{249}Cm	^{250}Cm	^{245}Bk	^{246}Bk
	^{247}Bk	^{248}Bk	^{249}Bk	^{250}Bk	^{246}Cf	^{248}Cf	^{249}Cf	^{250}Cf	^{251}Cf
	^{252}Cf	^{253}Cf	^{254}Cf	^{251}Es	^{252}Es	^{253}Es	^{254}Es	^{255}Es	^{55}Fm

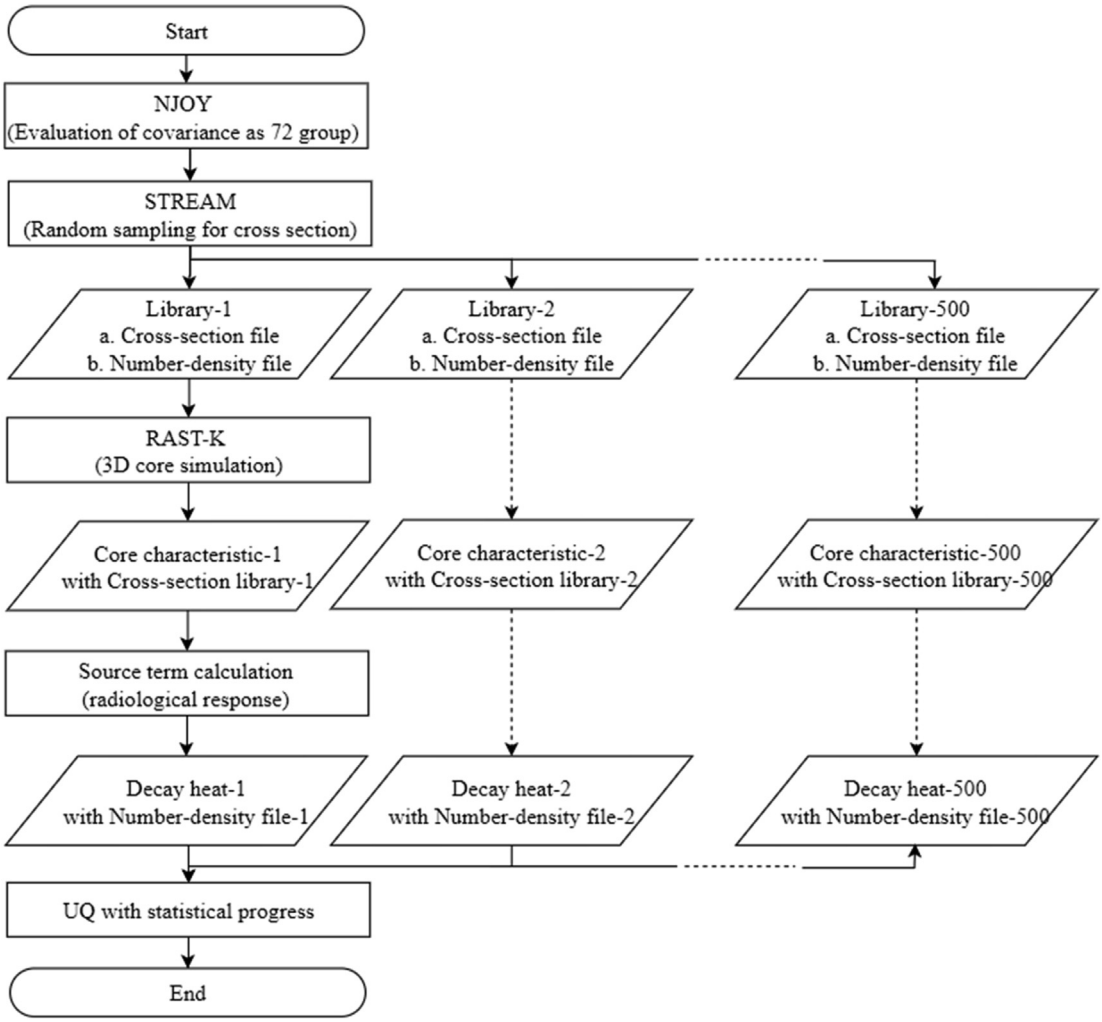

Fig. 1. Flow chart of UQ of decay heat calculation by two-step method.

that have covariance data of 144 isotopes in the ENDF/B-VII.1 library.

3. Description of FA sample

A B-43 benchmark sample is used for the analysis study in this paper. This section presents the specification of the B-43 FA discharged from Turkey Point-3. The decay heat of the FA is measured by the Handford Engineering Development Laboratory (HEDL) [13]. Table 2 introduces the measurement specifications: discharge burnup, cooling time, enrichment, FA type, and number of measurements. Fig. 2 displays the radial layout of the FA; B-43 has a

Table 2
Specification of FA problems.

Parameter	Value	Unit
Measurement Laboratory	HEDL	
Fuel assembly design	15 × 15	
Enrichment	2.6	w/o
Burnup	25.6	GWd/MTU
Cooling time	4.88	year
Fuel assembly pitch	21.50	cm
Rod pitch	1.430	cm
Clad thickness	0.0618	cm
Inlet temperature	558.7	K
Outlet temperature	611.0	K
Average soluble boron level	450	ppm
Number of fuel rods	204	
Number of instrument tube	1	
Number of guide tubes	20	
Effective fuel temperature	922	K
Operating day (2 cycles)	714 (cycle 01)/314 (cycle 02)	Day
Overhaul period	73	Day

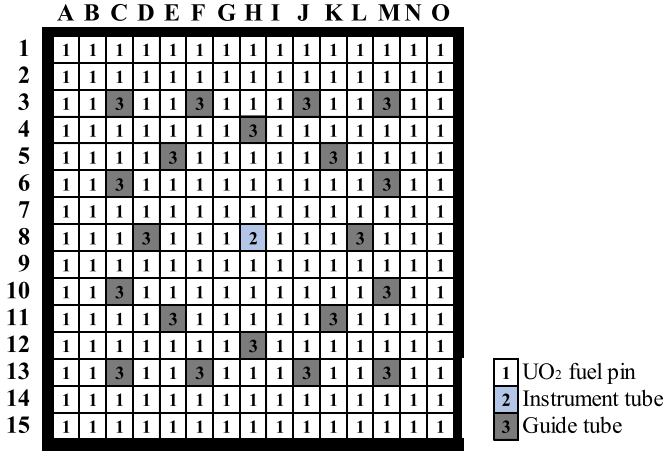

Fig. 2. Radial layout of B-43 FA

15 × 15 FA geometry and actinide (cobalt-60) is contained in the cladding material. Smeared cladding material (*i.e.*, mixed cobalt-60 and zircaloy) is used for the calculation.

4. Verification of decay heat uncertainty with STREAM-SNF

This section presents a code-to-code comparison to STREAM-SNF to assess the reliability of the decay heat results calculated by RAST-K SNF. STREAM-SNF is an analysis code system for SNF and has been validated with 91 decay heat measurements on 52 PWR FAs [22,26,27]. STREAM-SNF predicts the isotope inventory and its consequences (activities, decay heat, and neutron sources) to solve the micro-depletion chain using CRAM [14]. Table 3 lists the decay heat uncertainty of B-43 FA. The amount of decay heat uncertainty is similar to the scale values calculated by STREAM-SNF and RAST-K SNF. RAST-K SNF is used for analysis in this study.

5. Results and discussion

To evaluate the effect of the neutronics data and design parameters on the decay heat uncertainty, this section presents the sensitivity study results. Section 5.1 presents the calculated decay heat uncertainty results with ENDF/B-VII.1 covariance data. Section 5.2 discusses the effect of discharge burnup and cooling time on the decay heat uncertainty. Section 5.3 addresses the sensitivity study results according to the design parameters (*i.e.,* specific power density, moderator temperature, and fuel temperature) and operating conditions (*i.e.,* UO_2 enrichment, UO_2 density, and pellet radius). Section 5.4 presents the calculation results related to different parameters.

5.1. Decay heat uncertainty calculated using ENDF/B-VII.1 covariance data

Table 4 lists the decay heat uncertainty results for B-43. For the calculation, 500 perturbed neutronic data (*i.e.*, cross-section data and number-density file) were used. The average decay heat was calculated as 616.49 W. Compared to the measurement, the calculation result indicated a relative difference of −3.22%. The decay heat uncertainty was calculated to be 0.6488%. The average decay heat was calculated using Equation (5).

$$\overline{C} = \frac{\sum_{i=1}^{N} C_i}{N}, \tag{5}$$

where $\overline{C}$ is the average decay heat; N is the number of cross-section libraries (*i.e.*, 500), *and* C_i is the calculated decay heat with the ith cross-section library (*i.e.,* perturbed number-density file and two-group cross-section data with ith random seed). The decay heat uncertainty was calculated by dividing the standard deviation by the average decay heat of B-43, as indicated in Equation (6).

$$\text{Decay heat uncertainty} = \frac{\sigma_C\ [\text{W}]}{\overline{C}\ [\text{W}]} * 100\ \ [\%]\ , \tag{6}$$

where σ_C is the standard deviation of 500 calculated decay heats calculated using Equation (7).

$$\sigma_C = \sqrt{\frac{\sum_{i=1}^{N}\left(C_i - \overline{C}\right)}{N-1}}. \tag{7}$$

Fig. 3 presents the decay heat uncertainty of 18 isotopes that had a dominant effect on the total decay heat uncertainty. The decay heat uncertainty was calculated using Equation (8).

Table 3
Verification of decay heat uncertainty with STREAM-SNF as unit watt.

Reactor	FA ID	One standard deviation			Decay heat uncertainty		
		STREAM-SNF[a] [W]	RAST-K SNF[b] [W]	Absolute difference (R−S) [W]	STREAM-SNF [%]	RAST-K SNF [%]	Absolute difference (R−S) [%]
Turkey Point-3	B43	4.11	4.00	−0.11	0.6574	0.6490	−0.0084

a and *b* are decay heat uncertainty (one standard deviation) calculated by RAST-K SNF and STREAM-SNF, separately.

Table 4
Decay heat uncertainty of B-43.

FA ID	Enrichment [w/o]	Burnup [GWd/MTU]	Cooling period [years]	Measured decay heat [W]	ENDF/B-VII.1	
					Average decay heat [W]	Uncertainty [%]
B-43	2.6	25.595	4.882	637	616.49	0.6488

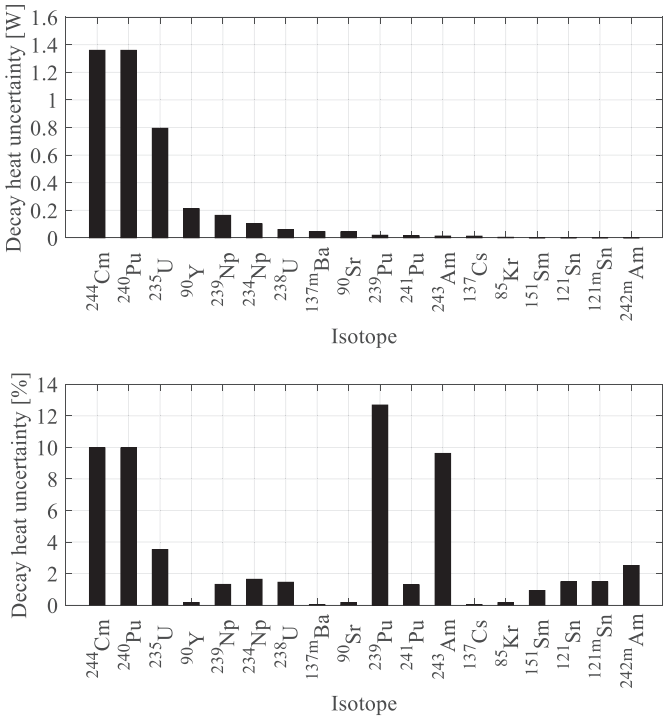

Fig. 3. Decay heat uncertainty of 18 isotopes.

where i is the isotope index; k is the perturbed library index; σ_C^i is the standard deviation of isotope i; N is the number of cross-section libraries (*i.e.*, 500); $\overline{C}^i$ is the average decay heat of isotope i, and C_k^i is the decay heat of isotope i with perturbed cross-section library with kth random seed. As indicated in Fig. 3, the ^{244}Cm, ^{240}Pu, ^{235}U, ^{90}Y, and ^{239}Np isotopes had a dominant effect on the decay heat uncertainty. The nuclides of ^{244}Cm, ^{240}Pu, ^{235}U, and ^{239}Np were directly influenced by the ENDF/B-VII.1 covariance data, and ^{90}Y was indirectly influenced by the covariance data. The nuclide of ^{90}Y was influenced by ^{89}Y through a neutron capture reaction; therefore, the amount of decay heat uncertainty was less than that of the other isotopes (*i.e.*, ^{244}Cm, ^{240}Pu, and ^{235}U).

Fig. 4 presents the distribution of the decay heats calculated using 500 perturbed neutronics data. To determine whether the decay heat data followed a normal distribution, the Shapiro–Wilk test was performed [28]. Because the p-value was greater than 0.05, the decay heat data of B-43 followed a normal distribution.

5.2. Discharge burnup and cooling period

This section presents the effect of the cooling period and discharge burnup on the decay heat uncertainty. Fig. 5 presents the isotope contribution in the decay heat according to the cooling period after discharge burnup of 28.5 GWd/MTU. Eleven dominant isotopes were compared: ^{241}Am, ^{137m}Ba, ^{90}Y, ^{238}Pu, ^{239}Pu, ^{240}Pu, ^{137}Cs, ^{90}Sr, ^{144}Pr, ^{106}Rh, and ^{134}Cs. The effects of ^{144}Pr, ^{106}Rh, and

$$\text{Decay heat uncertainty of isotope} = \frac{\sigma_C^i}{\overline{C}^i} * 100\ [\%] = \frac{\sqrt{\frac{\sum_{k=1}^{N}\left(C_k^i - \overline{C}^i\right)}{N-1}}}{\overline{C}^i} * 100\ [\%], \tag{8}$$

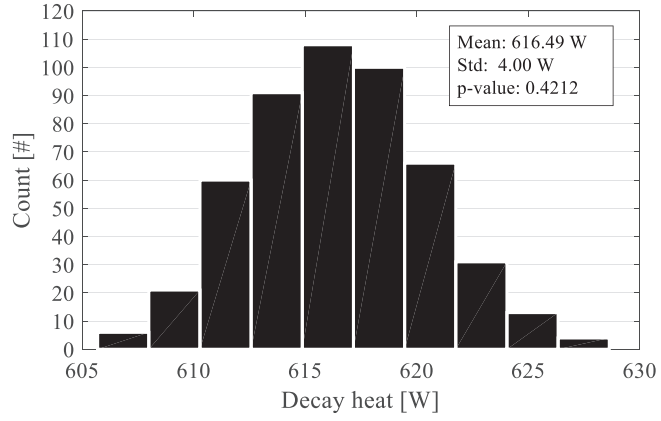

Fig. 4. Decay heat distribution of B-43 FA

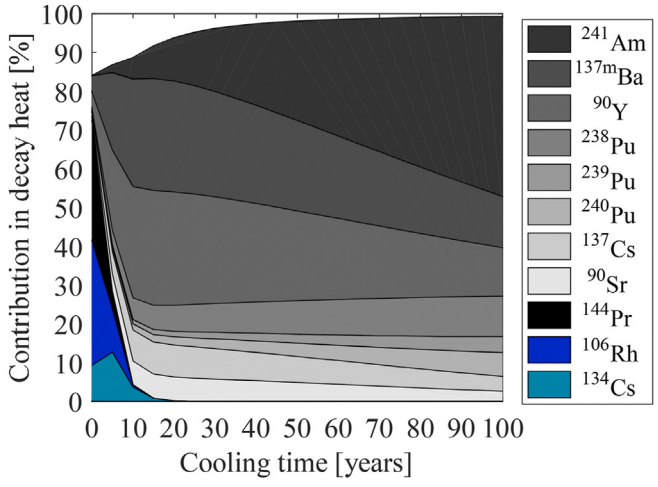

Fig. 5. Decay heat contribution of isotopes as a function of cooling time (B43 of Turkey Point-3).

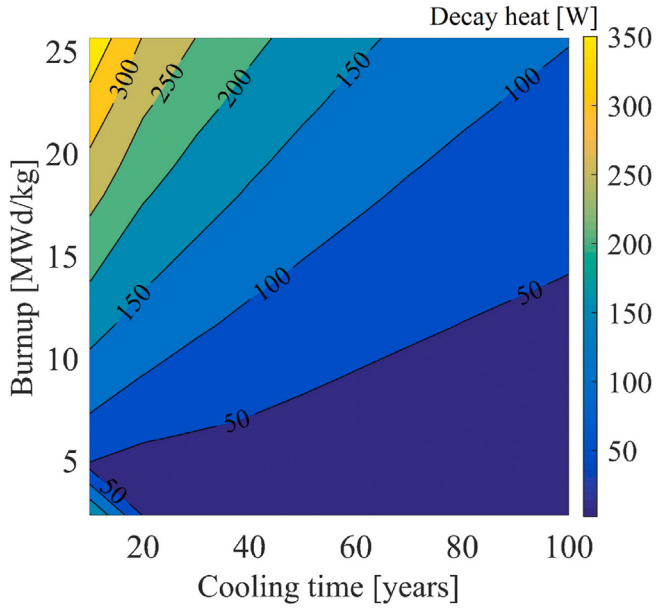

Fig. 6. Decay heat as a function of burnup and cooling time (Turkey Point-3, B-43).

^{134}Cs were dominant in the cooling range of 0 (discharge) to 100 years. After 10 years of cooling, the contribution of these three isotopes could be ignored, and the effects of ^{241}Am, ^{137m}Ba, and ^{90}Y were dominant. Approximately 70% of the decay heat was generated by these isotopes. The contribution of ^{241}Am in the decay heat increased as the cooling period increased.

Fig. 6 presents the decay heat as a function of both cooling period and discharged burnup with unit W. The calculation results were generated by the perturbed ENDF/B-VII.1 XS library. A sensitivity study was performed with a cooling period range of 0 (discharge) to 100 years, where results were obtained with 10-year cooling intervals. Ten burnup points were used for the sensitivity study: 2.31, 4.62, 6.93, 9.24, 11.55, 13.86, 17.94, 19.39, 22.29, and 25.60 MWd/kg. Therefore, 100 analysis points (*i.e.*, 10 cooling points multiplied by 10 burnup points) were used in this study. In addition, 500 perturbed two-group XS data and 500 perturbed ND files were used for the calculation of each analysis point. The ENDF/B-VII.1 covariance data perturbed 144 isotopes.

Fig. 7 presents the decay heat uncertainties of ^{244}Cm and ^{240}Pu. Fig. 8 displays the results for ^{235}U and ^{90}Y; Fig. 9 displays ^{239}Pu and ^{243}Am. The isotopes ^{244}Cm, ^{240}Pu, ^{235}U, and ^{90}Y had a dominant effect on the decay heat uncertainty, as indicated in Fig. 3. ^{239}Pu and ^{243}Am were dominant isotopes that had the greatest decay heat

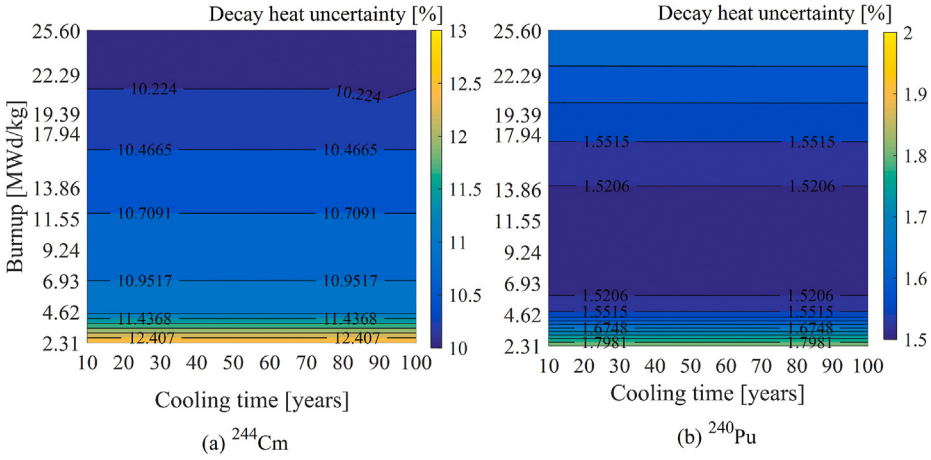

Fig. 7. Isotope uncertainty as a function of burnup and cooling time (^{244}Cm and ^{240}Pu).

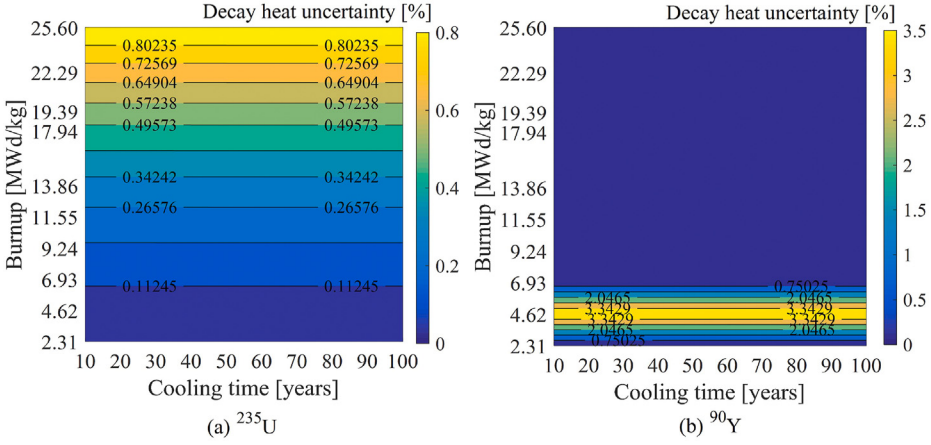

Fig. 8. Isotope uncertainty as a function of burnup and cooling time (^{235}U and ^{90}Y).

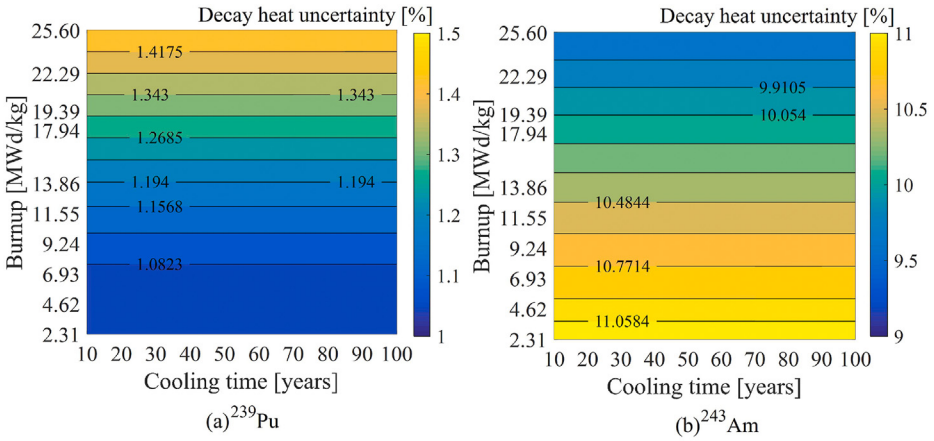

Fig. 9. Isotope uncertainty as a function of burnup and cooling time (^{239}Pu and ^{243}Am).

uncertainty as a unit percent. The decay heat uncertainty of the isotopes was calculated using Equation (8). Burnup had a dominant effect on the decay heat uncertainty of these six isotopes (*i.e.*, ^{244}Cm, ^{240}Pu, ^{235}U, ^{90}Y, ^{239}Pu, and ^{243}Am). In detail, the decay heat uncertainties of ^{244}Cm and ^{243}Am decreased as the burnup period proceeded, and the decay heat uncertainties of ^{235}U and ^{239}Pu increased as the burnup period proceeded. The decay heat uncertainty of ^{90}Y increased when less than a burnup of 6.93 MWd/kg and decreased when greater than a burnup of 6.93 MWd/kg. The decay heat uncertainty of ^{240}Pu decreased at less than 13.86 MWd/kg and increased at greater than 13.86 MWd/kg. In addition, the isotopes of ^{244}Cm, ^{240}Pu, ^{235}U, and ^{239}Pu were directly influenced by the ENDF/B-VII.1 covariance data, and the isotopes of ^{90}Y and ^{243}Am were indirectly influenced by the covariance data. The amount of ^{90}Y was influenced by ^{89}Y owing to the capture reaction, and the amount of ^{243}Am was influenced by the amount of ^{247}Bk according to alpha decay. Moreover, the six isotopes had the same trend as Fig. 3. B-43 FA was discharged at 25.6 MWd/kg and had a cooling period of 4.88 years. The decay heat uncertainty was compared at this point; ^{244}Cm, ^{240}Pu, ^{239}Pu, and ^{243}Am had a large decay heat uncertainty compared to ^{235}U and ^{90}Y.

5.3. Contribution of modeling parameters

5.3.1. Sensitivity study of operating conditions and FA design parameters

This section addresses the uncertainty caused by the FA design parameters and operating conditions. The B-43 FA of Turkey Point-3 was used for the calculation. The B-43 FA was irradiated in two cycles (*i.e.*, Cycles 1 and 2). The specific power conditions are presented in Table 5. An active height of 365.8 cm was used for the 3D nodal calculation [13], and the FA model was designed with a reflective boundary. In addition, the unperturbed ENDF/B-VII.1 XS library, unperturbed ENDF/B-VII.0 decay library, and a cooling period of 4.88 years were used for the calculation.

Table 5 lists the initial design parameters of the B-43 FA model. The uncertainty of the FA design and operating conditions are also included in this table [2]: UO_2 enrichment, UO_2 density, UO_2 pin diameter, specific power, moderator temperature, and fuel temperature. 1σ is the standard deviation of the parameters [2] and was used for the perturbed initial design variables. Table 6 presents the sensitivity of the design parameters and operating conditions. The UO_2 pin diameter had the greatest sensitivity compared to the other parameters.

Fig. 10 presents the sensitivity of the fuel design parameters and operating conditions. Sensitivity refers to the relative difference of

Table 6
Relative sensitivity with design parameters and operating conditions.

FA ID	Parameter	Sensitivity[a] (%)
B-43	Specific power	0.12
	Moderator temperature	0.22
	Fuel temperature	−0.02
	UO_2 Enrichment	−0.32
	UO_2 density	1.16
	UO_2 pin diameter	3.08

[a] is calculated by $\frac{Decay\ heat_{1\sigma\ change\ of\ parameter} - Decay\ heat_{origin}}{Decay\ heat_{origin}} * 100\ [\%]$, where value of decay $heat_{1\sigma\ change\ of\ parameter}$ is calculated decay heat with 1σ change of parameter and value of decay $heat_{origin}$ is calculated with original parameter.

Table 5
Uncertainty of operating condition and Spatial geometry for FA design.

Initial design variables[a]			Uncertainty		
Parameter	Value	Unit	1σ	Unit	PDF[b]
UO_2 enrichment	2.557	w/o	0.05	w/o	Normal
UO_2 density	10.19	g/cm^3	0.125	g/cm^3	Normal
UO_2 pin diameter	0.9296	cm	0.015	cm	Normal
Specific power	10.715 (cycle 1)	MW	1.67	%	Normal
	13.447 (cycle 2)	MW			
Moderator temperature	296.85	°C	3.33	%	Normal
Fuel temperature	648.85	°C	3.33	%	Normal

[a] Variables based on B-43 FA discharged from Turkey Point-3.
[b] PDF is probability density function and distribution of parameters.

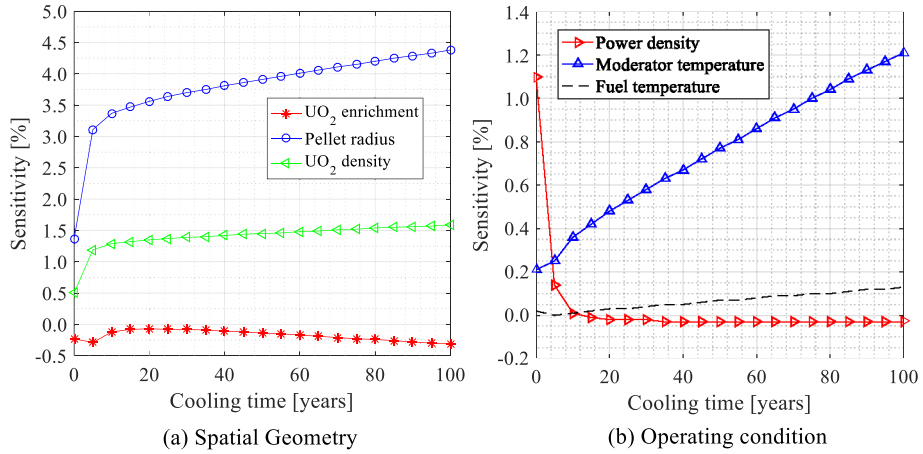

Fig. 10. Sensitivity as a function of cooling periods.

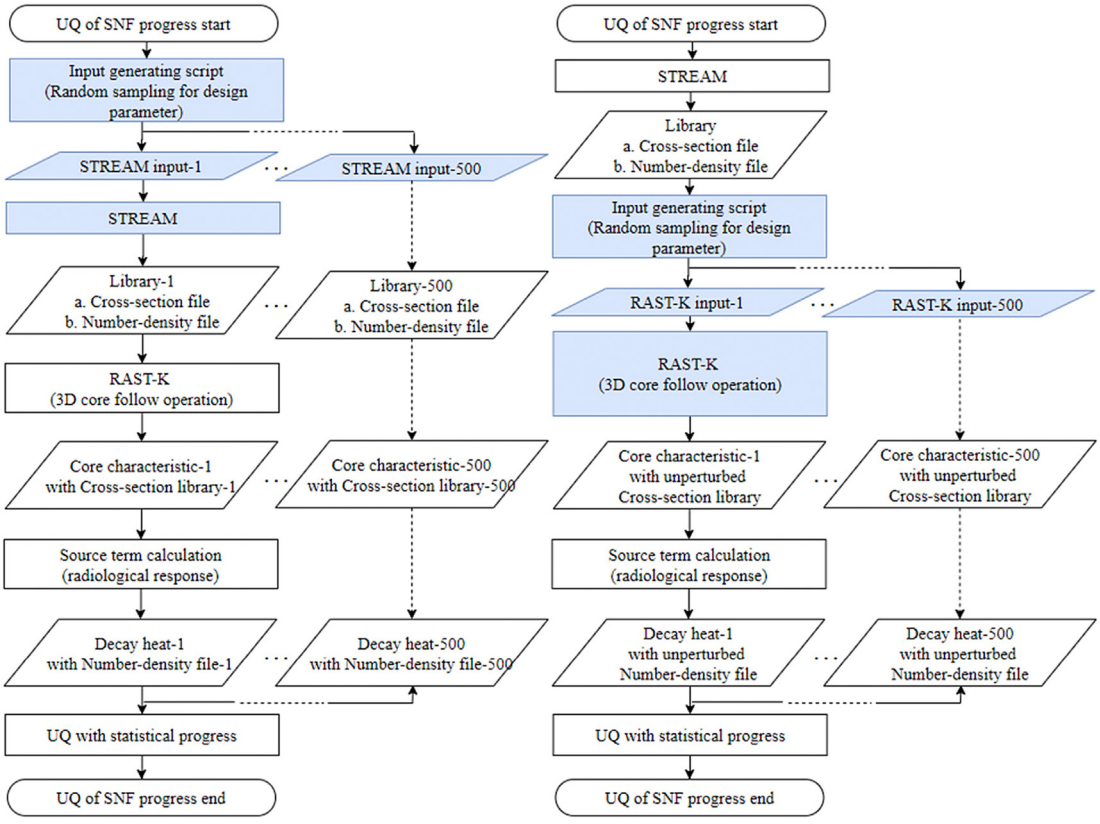

Fig. 11. Flow chart for perturbation of FA design parameters and operating conditions.

the decay heat when a parameter is changed by one standard deviation, as indicated in Fig. 10. For example, when the design parameter of the UO_2 enrichment was changed to 2.507 w/o from 2.557 w/o, the change in the decay heat was 1.16% of the initial value. The results were calculated as a function of the cooling period. A cooling interval of 5 years and 20 analysis points were used for the calculation. Subplot (a) contains the sensitivity results by design parameter and subplot (b) indicates the results obtained under the operating conditions. It can be observed that the decay heat had a higher sensitivity in the design parameters compared to the operating conditions.

5.3.2. Uncertainty of operating conditions and FA design parameters

This section presents the effect of the perturbed FA design parameters (*i.e.*, UO_2 enrichment, UO_2 density, pellet radius) and operating conditions (*i.e.*, moderator temperature, fuel temperature, and power density) on the decay heat uncertainty. Python was used to perturb each parameter with a random series [29]. A normal distribution was used for the probability density function (PDF) of each parameter, as mentioned in Table 5 [2]. Fig. 11 displays the flowchart of the stochastic sampling method with design parameters and operating conditions. Subplot (a) presents the calculation progress with perturbed design parameters generated by the Python

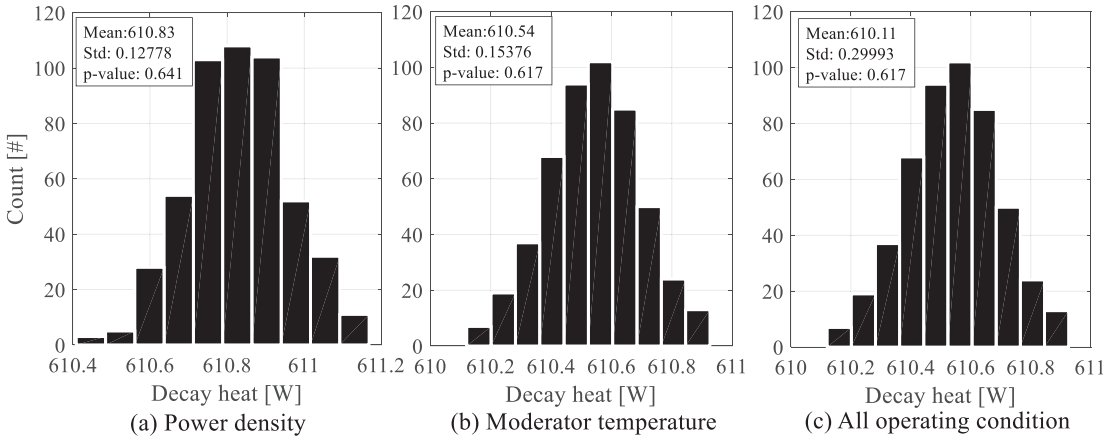

Fig. 12. Decay heat distribution with perturbed operating parameter.

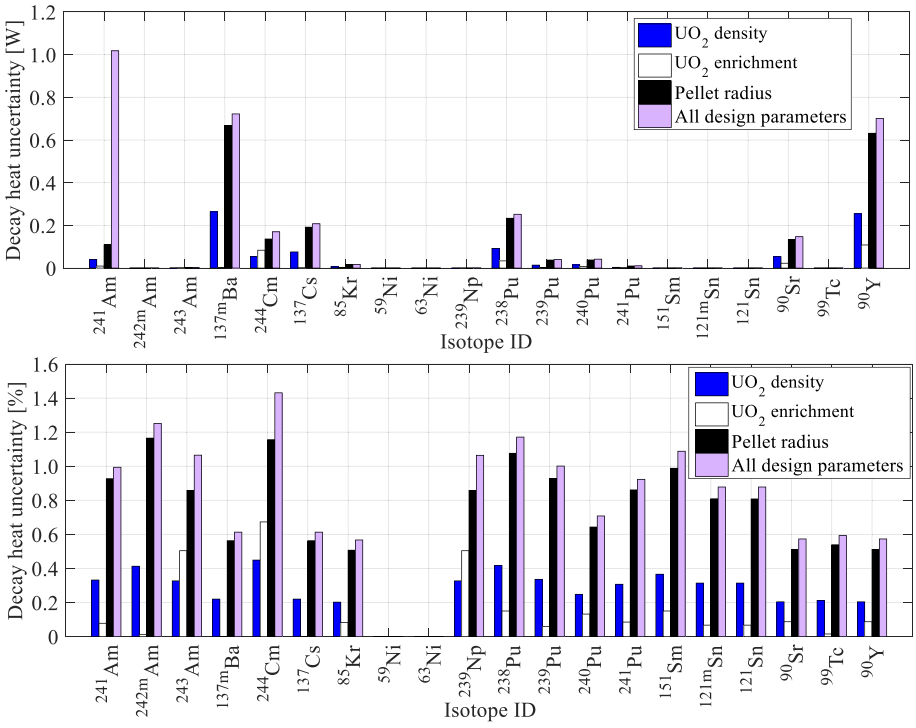

Fig. 13. Contribution of isotope uncertainty with perturbed FA design parameters.

script (input generating script). The script generated 500 STREAM inputs for the production of two-group XS libraries and ND files. The unperturbed ENDF/B-VII.1 XS library and unperturbed ENDF/B-VII.0 decay library were used for the calculation. The 3D nodal simulation was performed using the 500 perturbed libraries. Subplot (b) presents the progress with perturbed operating conditions using Python. In this case, the Python script generated 500 perturbed RAST-K inputs for the 3D core simulation. STERAM provided two-group cross-section and number-density files with unperturbed design parameters. The unperturbed ENDF/B-VII.1 cross-section library and unperturbed ENDF/B-VII.0 decay library were used in this calculation. Core-characteristic-1 to 500 represent the simulation results with the perturbed RAST-K inputs.

To assess whether the distribution of the calculated decay heat followed the normal distribution, the Shapiro–Wilk test was performed. Fig. 12 presents the distribution of the decay heats calculated by each operating condition with a p-value. All cases followed the normal distribution (*i.e.*, p-value > 0.05), and the mean values of the three distributions were the same as the nominal value.

Fig. 13 presents the isotope decay heat uncertainty. The decay heat uncertainty of the isotope was calculated using Equation (7). The nuclides ^{244}Cm and ^{90}Y had a dominant effect on the total decay heat uncertainty of the perturbed UO_2 enrichment. The isotopes ^{90}Y and ^{137m}Ba were dominant in the UO_2 density and pellet radius cases. The case of pellet radius had the greatest effect on the decay heat uncertainty; the UO_2 density case was the second most dominant parameter, and the UO_2 enrichment case indicated the least effect.

Fig. 14 displays the isotope decay heat uncertainty according to the perturbed operating conditions; three conditions are compared: power density, moderator temperature, and all operating conditions. In the case of all operating conditions, three

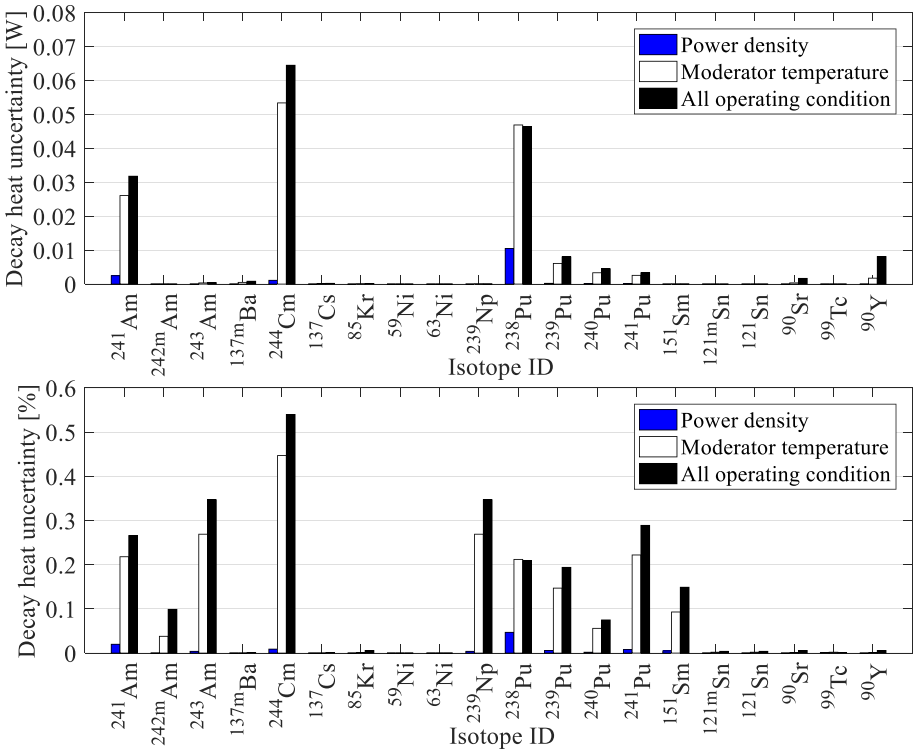

Fig. 14. Contribution of isotope uncertainty with perturbed operating conditions.

Table 7
Uncertainty for sensitivity study of B-43 FA discharged from Turkey Point-3.

Sensitivity study	Parameter	Uncertainty [W]	Uncertainty[a] [%]
Covariance data	ENDF/B-VII.1	4.00	0.65
Design parameter	UO_2 density	1.29	0.21
	UO_2 enrichment	0.28	0.05
	Pellet radius	3.28	0.53
	All design parameters	3.54	0.57
Operating condition	Moderator temperature	0.15	0.02
	Power	0.13	0.02
	All operating conditions	0.30	0.05

[a] is decay heat uncertainty calculated by Equation (8).

parameters (*i.e.*, power density, moderator temperature, and fuel temperature) were perturbed by one standard deviation of each operating condition, as indicated in Table 5. As displayed in Fig. 10 because the sensitivity of the fuel temperature was overly small (approximately zero), three perturbed operating conditions were used for the calculation rather than only the perturbed fuel temperature condition. The nuclides ^{241}Am and ^{238}Pu had a dominant effect on the decay heat uncertainty in the case of power. The isotopes ^{241}Am, ^{244}Cm, and ^{238}Pu were dominant in the moderator temperature case. The perturbed moderator temperature had a greater effect on the decay heat uncertainty compared to the perturbed specific power conditions.

5.4. Summary of parameter contribution to uncertainty

This section presents the effect of each parameter on the total decay heat uncertainty. The comparison model was B-43 FA discharged from Turkey Point-3.

Table 7 lists the decay heat uncertainties calculated by eight different parameters on three diverse groups. Fig. 15 presents the calculated decay heat uncertainties for each of the eight cases. The perturbed neutronic data had a dominant effect on the decay heat uncertainty compared to the operating conditions and design parameters. The pellet radius had a dominant effect on the design parameters. All cases had within a 1% contribution to the decay heat uncertainty.

6. Conclusion

UQ is an important issue for the long-term deposit management of SNF assemblies. The verification and validation of nuclear fuel analysis codes for licensing purposes must be accompanied by UQ related to different sources: nuclear data, assembly design, reactor core operating conditions, physical models, and numerical methods. In this work, we quantified the uncertainty of the depleted light-water FA B-43 of the Turkey Point-3 benchmark and analyzed the partial contribution of several sources to the total uncertainty of an FA's decay heat.

The UQ algorithm included a random sampling of the FA input data and calculation of every sample by a two-step analysis code system comprising the lattice code STREAM, nodal code RAST-K, and SNF module. Overall, the sampling of the nuclear data was

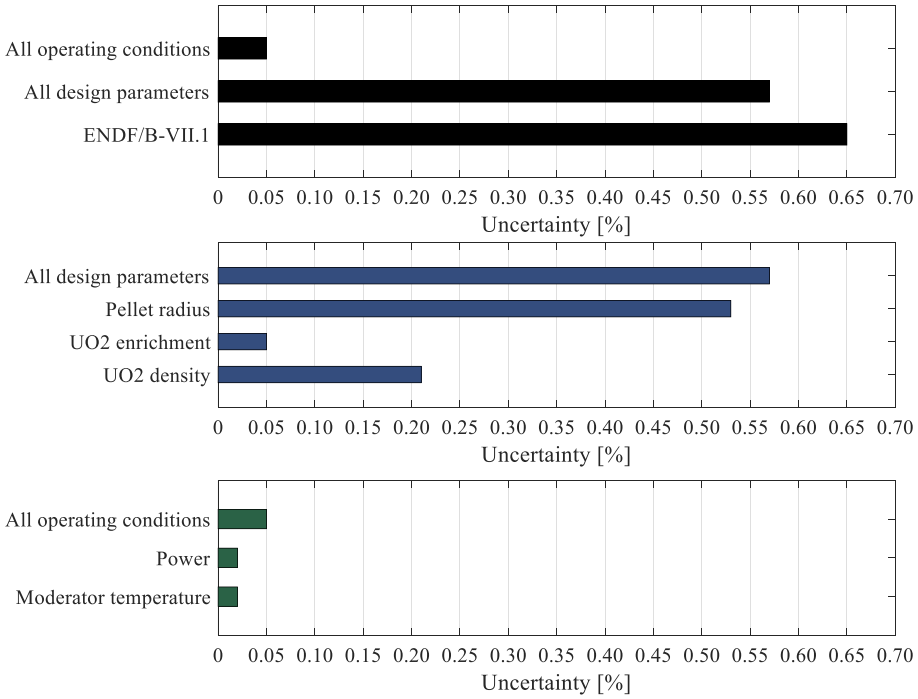

Fig. 15. Contribution of decay heat uncertainty with different parameters of B-43 FA discharged from Turkey Point-3.

based on the 72-group micro cross-section covariance matrices evaluated by NJOY for 144 isotopes of ENDF/B-VII.1. STREAM performed a series of steady-state fuel assemblies of different design parameters, burnup, power, and inlet coolant temperature for all the generated multi-group library samples. The resulting data set was collapsed into the number of two-group cross-section libraries and isotope number-density files used by RAST-K to produce the decay heat and isotopic inventory changes during a cooling period. Subsequently, the calculated output data underwent a statistical and sensitivity investigation to analyze the components and trend of the decay heat uncertainty at different cooling time moments and fuel burnups.

The uncertainty analysis of the FA under consideration demonstrated that the decay heat uncertainty decreased with the cooling time. Nuclear data and assembly design parameters were the greatest contributors to the total decay heat uncertainty accounting for 0.7% and 0.5%, respectively, whereas the reactor core power and inlet coolant temperature contributions were less than 0.1%. The majority of the decay heat uncertainty was propagated by the medium of several isotopes: ^{241}Am, ^{137}Ba, ^{244}Cm, ^{238}Pu, ^{134}Cs, and ^{90}Y.

In the future, we plan to use the two-step analysis code system STREAM/RAST-K for the nuclear safety analysis of spent nuclear fuel assembly discharged from a Korean pressurized water reactor core, and uncertainty quantification due to fission product yield will be performed based on various libraries.

Declaration of competing interest

The authors declare that they have no known competing financial interests or personal relationships that could have appeared to influence the work reported in this paper.

Acknowledgments

This work was supported by the National Research Foundation of Korea (NRF) grant funded by the Korea government (MSIT). (No.NRF-2019M2D1A1067205)

Abbreviations

1D	one-dimensional
2D	two-dimensional
3D	three-dimensional
BOR	boron concentration
BWR	boiling water reactor
CMFD	coarse mesh finite difference
CRAM	Chebyshev rational approximation method
EOC	end of cycle
FA	fuel assembly
HEDL	Hanford Engineering Development Laboratory
ND	number density
PCF	power correction factor
PSM	point energy slowing-down method
PWR	pressurized water reactor
RK	RAST-K v2.0
SFP	spent fuel pools
SNF	spent nuclear fuel
ST	STREAM
TFU	fuel temperature
TH1D	one-dimensional thermal-hydraulic feedback
TMO	moderator temperature
UNM	unified nodal method
W/O	weight percent
XS	cross-section

Appendix

Table A1 to Table A4 contain the decay heat uncertainty of B-43 FA according to burnup and cooling periods. A comparison of 100 analysis points is performed.

Table A1
Decay heat uncertainty according to burnup and cooling periods I

Burnup [MWd/kg]	2.31			4.62			6.93		
Cooling period [years]	Total decay heat [W]	Uncertainty		Total decay heat [W]	Uncertainty		Total decay heat [W]	Uncertainty	
		[W]	[%]		[W]	[%]		[W]	[%]
10	201.554	5.603	2.78	43.556	0.480	1.10	93.892	0.205	0.22
20	47.316	1.647	3.48	27.208	0.239	0.88	70.985	0.151	0.21
30	14.154	0.440	3.11	21.130	0.159	0.75	57.557	0.138	0.24
40	5.317	0.114	2.15	17.478	0.126	0.72	47.554	0.133	0.28
50	2.888	0.034	1.20	14.854	0.109	0.73	39.737	0.131	0.33
60	2.196	0.021	0.99	12.825	0.097	0.76	33.538	0.129	0.39
70	1.984	0.020	1.05	11.215	0.088	0.79	28.598	0.128	0.45
80	1.909	0.020	1.08	9.925	0.082	0.83	24.656	0.127	0.51
90	1.873	0.020	1.10	8.887	0.077	0.87	21.505	0.125	0.58
100	1.849	0.020	1.11	8.051	0.073	0.91	18.984	0.124	0.65

Table A2
Decay heat uncertainty according to burnup and cooling periods II

Burnup [MWd/kg]	9.24			11.55			13.86		
Cooling period [years]	Total decay heat [W]	Uncertainty		Total decay heat [W]	Uncertainty		Total decay heat [W]	Uncertainty	
		[W]	[%]		[W]	[%]		[W]	[%]
10	132.332	0.222	0.17	167.499	0.313	0.19	202.283	0.429	0.21
20	101.481	0.189	0.19	129.202	0.268	0.21	156.399	0.362	0.23
30	83.024	0.196	0.24	106.470	0.280	0.26	129.580	0.375	0.29
40	69.104	0.201	0.29	89.253	0.288	0.32	109.241	0.383	0.35
50	58.151	0.204	0.35	75.648	0.291	0.38	93.122	0.387	0.42
60	49.426	0.205	0.41	64.769	0.292	0.45	80.196	0.386	0.48
70	42.448	0.204	0.48	56.038	0.290	0.52	69.791	0.383	0.55
80	36.860	0.202	0.55	49.022	0.287	0.59	61.405	0.379	0.62
90	32.380	0.200	0.62	43.377	0.284	0.65	54.637	0.373	0.68
100	28.784	0.198	0.69	38.830	0.280	0.72	49.167	0.368	0.75

Table A3
Decay heat uncertainty according to burnup and cooling periods III

Burnup [MWd/kg]	17.943			19.392			22.291		
Cooling period [years]	Total decay heat [W]	Uncertainty		Total decay heat [W]	Uncertainty		Total decay heat [W]	Uncertainty	
		[W]	[%]		[W]	[%]		[W]	[%]
10	265.578	0.707	0.27	286.646	0.832	0.29	331.222	1.164	0.35
20	204.902	0.575	0.28	221.822	0.669	0.30	256.533	0.909	0.35
30	170.682	0.577	0.34	185.183	0.660	0.36	214.572	0.859	0.40
40	144.803	0.578	0.40	157.380	0.656	0.42	182.715	0.832	0.46
50	124.262	0.576	0.46	135.274	0.650	0.48	157.372	0.811	0.52
60	107.740	0.570	0.53	117.473	0.641	0.55	136.951	0.792	0.58
70	94.396	0.562	0.60	103.083	0.630	0.61	120.427	0.773	0.64
80	83.599	0.553	0.66	91.427	0.618	0.68	107.027	0.755	0.71
90	74.849	0.543	0.73	81.972	0.606	0.74	96.139	0.738	0.77
100	67.745	0.533	0.79	74.285	0.594	0.80	87.269	0.721	0.83

Table A4
Decay heat uncertainty according to burnup and cooling periods IV

Burnup [MWd/kg]	25.596		
Cooling period [years]	Total decay heat [W]	Uncertainty	
		[W]	[%]
10	385.802	1.725	0.45
20	297.455	1.299	0.44
30	248.650	1.157	0.47
40	211.794	1.076	0.51
50	182.548	1.023	0.56
60	159.011	0.984	0.62
70	139.969	0.952	0.68
80	124.523	0.923	0.74
90	111.961	0.898	0.80
100	101.715	0.874	0.86

References

[1] Status of spent fuel storage for the first quarter of 2019 [Online]. (Available from: http://www.khnp.co.kr/board/BRD_000179/boardView.do?pageIndex=1&boardSeq=70138&mnCd=FN051304&schPageUnit=10&searchCondition=0&searchKeyword=, 2019e. Accessed on April 2019.

[2] G. Ilas, Liljenfeldt H, Decay heat uncertainty for BWR used fuel due to modeling and nuclear data uncertainties, Nucl. Eng. Des. 319 (2017) 176–184, https://doi.org/10.1016/j.nucengdes.2017.05.009.

[3] J. Jang, B. Ebiwonjumi, W. Kim, J. Park, J. Choe, D. Lee, Validation of spent nuclear fuel decay heat calculation by a two-step method, Nucl. Eng. Technol. (2021), https://doi.org/10.1016/j.net.2020.06.028.

[4] J. Jang, B. Ebiwonjumi, W. Kim, A. Cherezov, J. Park, D. Lee, Validation of Isotope Inventory Prediction for Back-End Cycle Management by Two-step Method, 2021, https://doi.org/10.1016/j.net.2021.01.009.

[5] O. Leray, D. Rochman, P. Grimm, H. Ferroukhi, A. Vasiliev, M. Hursin, G. Perret, A. Pautz, Nuclear data uncertainty propagation on spent fuel nuclide compositions, Ann. Nucl. Energy 94 (2016) 603–611, https://doi.org/10.1016/j.anucene.2016.03.023.

[6] N. García-Herranz, O. Cabellos, J. Sanz, J. Juan, J.C. Kuijper, Propagation of statistical and nuclear data uncertainties in Monte Carlo burn-up calculations, Ann. Nucl. Energy 35 (2008) 714–730, https://doi.org/10.1016/j.anucene.2010.06.006.

[7] D. Rochman, A. Vasiliev, H. Ferroukhi, T. Zhu, S.C. van der Marck, A.J. Koning, Nuclear data uncertainty for criticality-safety: Monte Carlo vs. linear perturbation, Ann. Nucl. Energy 92 (2016) 150–160, https://doi.org/10.1016/j.anucene.2016.01.042.

[8] M.B. Chadwick, et al., ENDF/B-VII.1 nuclear data for science and technology: cross sections, covariances, fission product yields and decay data, Nucl. Data Sheets 112 (12) (2011) 2887–2996, https://doi.org/10.1016/j.nds.2011.11.002.

[9] Ornl, SCALE: A Modular Code System for Performing Standardized Computer Analyses for Licensing Evaluations, ORNL/TM-2005/39, Version 6, vol. 4, 2009.

[10] N. García-Herranz, O. Cabellos, J. Sanz, Applicability of the MCNP–ACAB system to inventory prediction in high burn-up fuels: sensitivity/uncertainty estimates, in: Proc. Int. Conf. on Mathematics and Computation, M&C2005, Avignon, France, 2005.

[13] Validation of SCALE 5 Decay Heat Prediction for LWR Spent Nuclear Fuel. U.S.: U.S. National Regulatory Commission, NUREG/CR-6972, 2010.

[14] S. Choi, C. Lee, D. Lee, Resonance treatment using pin-based pointwise energy slowing-down method, J. Comput. Phys. 330 (2017) 134–155.

[15] J. Choe, S. Choi, P. Zhang, J. Park, W. Kim, H.C. Shin, H.S. Lee, J. Jung, D. Lee, Verification and validation of STREAM/RAST-K for PWR analysis, Nucl. Eng. Technol. 51 (2) (2019) 356–368.

[16] R.J.J. Stamm'ler, M.J. Abbate, Methods of Steady-State Reactor Physics in Nuclear Design, Academic Press, London, 1983.

[17] A. Yamamoto, K. Kinoshita, T. Watanabe, T. Endo, Uncertainty quantification of LWR core characteristics using random sampling method, Nucl. Sci. Eng. 181 (2015) 160–174, https://doi.org/10.13182/NSE14-152.

[18] R. Arcilla, et al., Processing neutron cross section covariances using NJOY-99 and PUFF-IV, Nucl. Data Sheets 109 (12) (2008) 2910–2914, https://doi.org/10.1016/j.nds.2008.11.033.

[19] D. Smith, Evaluated nuclear data covariances: the journey from ENDF/B-VII.0 to ENDF/BVII.1, Nucl. Data Sheets 112 (12) (2011) 3037–3053, https://doi.org/10.1016/j.nds.2011.11.004.

[20] P. Talou, P. Young, T. Kawano, et al., Quantification of uncertainties for evaluated neutron-induced reactions on actinides in the fast region, Nucl. Data Sheets 112 (12) (2011) 3054–3074, https://doi.org/10.1016/j.nds.2011.11.005.

[21] S. Hoblit, Y.-S. Cho, M. Herman, et al., Neutron cross section covariances for structural materials and fission products, Nucl. Data Sheets 112 (12) (2011) 3075–3097, https://doi.org/10.1016/j.nds.2011.11.006.

[22] B. Ebiwonjumi, S. Choi, M. Lemaire, D. Lee, H.C. Shin, H.S. Lee, Verification and validation of radiation source term capabilities in STREAM, Ann. Nucl. Energy 124 (2019) 80–87, https://doi.org/10.1016/j.anucene.2018.09.034.

[23] A. Quarteroni, R. Sacco, F. Saleri, Numerical Mathematics, 2007.

[24] S. Børresen, T. Bahadir, M. Kruners, Validation of CMS/SNF Calculations against Preliminary CLAB Decay Heat Measurements, Transactions of the American nuclear society, Omni Shoreham Hotel Washington, D.C, 2004. November 14-18.

[25] S. Børresen, Spent fuel analyses based on in-core fuel management calculations, in: Proc. of the PHYSOR 2004, The Physics of Fuel Cycles and Advanced Nuclear Systems: Global Developments, Chicago, Illinois, 2004. April 25-29.

[26] B. Ebiwonjumi, S. Choi, M. Lemaire, D. Lee, H.C. Shin, Lee Hs, Validation of lattice physics code STREAM for predicting pressurized water reactor spent nuclear fuel isotopic inventory, Ann. Nucl. Energy 120 (2018) 431–449, https://doi.org/10.1016/j.anucene.2018.06.002.

[27] B. Ebiwonjumi, C. Kong, P. Zhang, A. Cherezov, D. Lee, Uncertainty quantification of PWR spent fuel due to nuclear data and modelling parameters, Nucl. Eng. Technol. (2021), https://doi.org/10.1016/j.net.2020.07.012.

[28] R. Ihaka, R. Gentleman, R: a language for data analysis and graphics, J. Comput. Graph Stat. 5 (3) (1995) 299–314.

[29] M. Matsumoto, T. Nishimura, Mersenne Twister: a 623-dimensionally equidistributed uniform pseudorandom number generator, ACM Trans. Model Comput. Simulat 8 (1) (1998). January pp.3–30.